Article:
Galloway, AF, Akhtar, J, Marcus, SE et al. (2020) Cereal root exudates contain highly structurally complex polysaccharides with soil-binding properties. The Plant Journal, 103 (5). tpj.14852. pp. 1666-1678. ISSN: 0960-7412

https://doi.org/10.1111/tpj.14852

Cereal root exudates contain highly structurally complex polysaccharides with soil-binding properties

Andrew F. Galloway*, Jumana Akhtar*, Susan E Marcus, Nathan Fletcher, Katie Field, and Paul Knox#

*These authors contributed equally to the work

Centre for Plant Sciences, Faculty of Biological Sciences, University of Leeds, Leeds, LS2 9JT, UK.

For correspondence (email: j.p.knox@leeds.ac.uk).

Running Title: Cereal root exudate polysaccharides

Key words

Plant-soil interactions, root exudates, rhizosheaths, polysaccharides, *Triticum aestivum*, *Zea mays*

Summary

Rhizosheaths function in plant-soil interactions and are proposed to form due to a mix of soil particle entanglement in root hairs and the action of adhesive root exudates. The soil-binding factors released into rhizospheres to form rhizosheaths have not been characterised. Analysis of the high molecular weight root exudates of both wheat and maize plants indicate the presence of complex, highly branched polysaccharide components with a wide range of galactosyl, glucosyl and mannosyl linkages that do not directly reflect cereal root cell wall polysaccharide structures. Periodate oxidation indicates that it is the carbohydrate components of the high molecular weight exudates that have soil-binding properties. The root exudates contain xyloglucan (LM25), heteroxylan (LM11/LM27) and arabinogalactan-protein epitopes (LM2) epitopes and sandwich-ELISA evidence indicates that, in wheat particularly, these can be interlinked in multi-polysaccharide complexes. Using wheat as a model, exudate-binding monoclonal antibodies have enabled the tracking of polysaccharide release along root axes of young seedlings and their presence at root hair surfaces and in rhizosheaths. The observations indicate that specific root exudate polysaccharides, distinct from cell wall polysaccharides,

are adhesive factors secreted by root axes and that they contribute to the formation and stabilization of cereal rhizosheaths.

INTRODUCTION

The interface between plant roots and soils is highly complex. Roots extend into soils that are highly heterogeneous substrates in terms of mechanical properties, chemistry and water/nutrient availability. Root systems anchor plants in soils and access water and nutrients through developmentally plastic root architectures that also dynamically interact with soil biota. Roots influence the biology and chemistry of surrounding zones of soil known as rhizospheres (Walker et al. 2003; Rabbi et al. 2018). It is well established that roots release exudates that includes a range of low and high molecular weight (HMW) compounds which are likely to influence a wide range of soil properties (Walker et al. 2003; Naveed et al. 2017). In some cases, and particularly at root apices, roots exude polysaccharide-rich mucilage that is proposed to act as a lubricant to aid root penetration and to act in defence processes. In some instances, this is associated with the complete release of root cap cells, known as border cells, which remain physiologically active (Koroney et al. 2016).

In many cases, and particularly for grasses, root activities can lead to the formation of a coating of soil that is adhered to root structures known as a rhizosheath (Watt et al. 1994; George et al. 2014; Delhaize et al. 2015; Brown et al. 2017; Pang et al. 2017). Rhizosheaths are proposed to form and be stabilised through the action of soil particle entanglement with root hairs and adhesive mucilage, however the adhesive molecules at root surfaces have not been identified and structurally elucidated (Brown et al. 2017; Pang et al. 2017). Plant factors released into soil are likely to have a wide range of functions that would include altering soil biophysical factors, soil particle aggregation and the generation of microhydrological and microbiotic niches (Guinel and McCully 1986; Watt et al., 1993; Knee et al. 2001; Naveed et al. 2017; Benard et al. 2019). Factors involved in the maintenance of rhizosheaths may increase soil quality in general by increasing water flow and thus nutrient flow and soil aeration through more frequent pores (Tisdall and Oades 1982; Benard et al. 2019). During periods of drought, some grasses can increase the thickness of their rhizosheath, potentially in an effort to secure water uptake (Watt et al. 1994; Rabbi et al. 2018; Liu et al., 2019).

Basic understanding of the molecular factors that underpin the integrity of rhizosheaths is lacking. Root exudates include a wide range of molecular components and have been estimated to account for over 20% of photosynthetically fixed carbon (Walker et al. 2003; Naveed et al. 2017). However, the proportion of this that is high molecular weight molecules is not clear. Root mucilages arising from root apices have been characterised from only a few species and generally contain an array of molecular features equivalent to those found in cell wall polysaccharides (e.g. Bacic et al. 1986; Moody et al. 1988; Chaboud and Rougier, 1990; Knee et al. 2001; Koroney et al. 2016). Little is known of the cellular and physiological processes underpinning the release of polysaccharides or their properties and roles in rhizospheres and rhizosheath formation. Indeed, the release of polysaccharide exudates from regions other than root tips is proposed but has not been determined due to the technical challenges involved (Oburger and Jones 2018).

Monoclonal antibodies (MAbs) are sensitive and versatile reagents to track plant polysaccharides. Using sets of polysaccharide-directed MAbs, recent work has identified that a range of soluble polysaccharides are released from roots when plants are grown hydroponically and this has in turn led to the identification of the cell wall polysaccharide xyloglucan as being widely released from land plants (Galloway et al. 2018). Moreover, using tamarind seed xyloglucan as a proxy for root-exuded xyloglucan, evidence indicates that xyloglucan and other polysaccharides of plant and microbial origin have strong soil-binding properties and can act to promote soil particle aggregation (Galloway et al. 2018; Akhtar et al. 2018). While these findings represent an advancement in wider understanding of HMW root exudates, questions remain regarding their biochemical composition and structure and the potential for release of HMW exudates from regions other than root tips including the surface of root axes. Here, we address these knowledge gaps with a study of wheat and maize root exudates, two crop species with a strong capacity to form rhizosheaths. We demonstrate that roots of both species release broadly similar structurally complex polysaccharides with soil-binding properties. Known carbohydrate epitopes are present in the exudate polysaccharides. With a focus on wheat roots, the use of the cognate MAbs have been used to demonstrate polysaccharide release along the root axis of seedlings and their presence at the root-soil interface of rhizosheaths.

RESULTS

Wheat and maize roots release soil-binding high molecular weight exudates that contain a wide range of monosaccharide linkages

Wheat (cv. Cadenza) and maize (cv. Earlibird) were selected for a study of HMW polysaccharides in root exudates. Both species have a strong capacity to form rhizosheaths as shown in supplemental information. To study the polysaccharides released from wheat and maize roots, seedlings were grown in hydroponic systems in half-strength Hoagland nutrient solution. After this time, HMW compounds (>30,000 MW) were isolated from the growth media. Across a range of experiments, wheat and maize seedlings had released, at the point of collection, in the range of 1.5 to 2.0 mg HMW compounds / g root fresh weight. Total carbohydrate and protein analyses indicated that wheat HMW exudates were ~45% (w/w) carbohydrate and those of maize ~20% (w/w) carbohydrate. The soil-binding properties of wheat and maize HMW preparations have been reported previously using a nitrocellulose-based assay (Akhtar et al. 2018). Using this assay and a periodate oxidation treatment of HMW materials bound to nitrocellulose prior to the assay confirmed that carbohydrate components were required for the soil binding properties (Fig. 1).

Monosaccharide linkage analyses of the wheat and maize HMW preparations from hydroponic systems are shown in Table 1. There was a broad similarity between the wheat and maize samples. The major feature of the analyses for both species is the presence of an extremely wide range of sugar linkages with over 50 distinct linkages. Key features include the high proportion (50 - 60%) of terminal glycosyl residues (involving all of the monosaccharides detected other than galactopyranuronosyl residues) indicating extensive single residue substitutions of backbone residues. The most abundant terminal residues were galactopyranosyl linkages and these contributed ~20% of all linkages for the maize samples and ~10% for the wheat samples. Additionally, galactofuranosyl residues were detected in all samples. Features of heteromannan, heteroxylan, xyloglucan, AGPs and extensin are present (Table 1) but assignments of detected glycosyl signatures to plant cell wall polysaccharides are not possible for all linkages detected. A wide range of linkages was particularly the case for galactosyl, glucosyl and mannosyl residues. In the case of mannosyl residues 14 distinct linkages were detected across the samples and accounted for ~17% of the exudate glycan in both cases. In the case of glucosyl residues 12 different linkages were

detected and overall they accounted for in the region of ~30% of all sugars present. It is the diversity of carbohydrate linkages across all analyses that is of note here, and any differences between the species would appear to be marginal. Root-tip released polysaccharides are generally related to those found in plant cell walls and notable absences are pectic polysaccharides with only a very low abundance of linkage signatures indicative of the pectic polysaccharides homogalacturonan and rhamnogalacturonan-I.

Glycan epitope mapping of wheat and maize HMW root exudates with MAbs

To further characterise the polysaccharides of the HMW components of root exudates we glycan epitope mapped the materials with a wide range of monoclonal antibodies (MAbs) directed to plant cell wall glycans using ELISAs and as informed by the structural analyses. The two species had very similar epitope profiles for the exudates (Fig. 2). There were strong signals for xyloglucan and heteroxylan and also for some glycoprotein epitopes. In the case of heteroxylan, a strong signal was detected for the MAb LM11 that binds to 1,4-xylan but weaker signals for MAb LM10 (that is now known to recognise the non-reducing end of 1,4-xylan (Ruprecht et al. 2017)) and also for the glucuronoxylan MAb LM28. The strongest signal amongst heteroxylan-related MAbs was observed for LM27 that binds to a grass xylan associated epitope of unknown structure (Cornuault et al. 2015). Outside of heteroxylan and xyloglucan, the only epitopes to be detected at absorbances 0.1 au above background were glycoprotein epitopes. The LM2 AGP epitope was detected in all samples and the JIM13 AGP epitope detected in wheat albeit at a low level. The LM1 extensin epitope was detected in wheat exudates but only at a very low level in maize exudates.

In relation to the wide occurrence of diversely linked glucosyl residues there was no signal from probes for β-1,3-glucan (callose) or mixed-linkage glucan. Similarly, even though mannosyl residues were abundant in the samples there was no recognition by any mannosyl probes tested including MAbs LM21 and CCRC-170 nor the mannan-directed CBM27. Confirming the absence of significant linkages assigned to pectic polysaccharides in the structural analyses, no epitopes of rhamnogalacturonan-I or xylogalacturonan were detected and there was only a weak signal with LM19 for homogalacturonan in the wheat samples (Fig. 2).

Given the distinct profiles and potential complexity of polysaccharides in HMW root exudates it would be of interest to determine if any of the identified glycan epitopes are interlinked within exudate macromolecules. Sandwich-ELISA was performed with xylan-binding CBM2b1-2 as the capture molecule (alongside mannan-binding CBM27 a non-binding CBM). Following incubation with HMW materials at 10 µg/mL potential complexes were probed with MAbs. There is strong evidence for xylan linking to xyloglucan and AGP in the wheat exudates suggestive of the presence of multi-polysaccharide complexes as shown in Fig. 3. However, the evidence for multi-polysaccharide complexes was less conclusive for the maize samples.

Glycan epitopes of root exudates are released along wheat root axes

In light of the observations reported above and with generally higher level of epitopes in wheat root exudate HMW compounds we focused on the wheat root system for further analysis using MAbs. To gain insight into where the exudate polysaccharides are released from wheat roots, the major epitopes binding to known structural features present in the exudates were tracked after wheat seedlings had been placed on nitrocellulose sheets for just 2 h before removal and probing of the sheets with MAbs. Examples of the patterns of release of the LM25 xyloglucan, LM11 xylan and LM2 AGP epitopes in the 2 h period are shown in Fig. 4. All three epitopes were readily detected on the nitrocellulose sheet and marked the length of the root axes and not just the root tips. A root print pattern for an irrelevant non-binding MAb and a print with a seedling pre-treated with formaldehyde fixative prior to seedling transfer to a nitrocellulose sheet are shown (Fig. 4). This indicates the specificity of epitope release from the root axis of living seedlings. Additionally, the soil adhesion assay protocol (Akhtar et al. 2018) was applied to nitrocellulose sheets that had been printed with a living seedling for 2 h and, although not as consistent as epitope detection, clear signals for soil adhesion were observed marking where the roots had been (Fig. 4). The printing, on nitrocellulose for only 10 min, of larger root systems that had been grown hydroponically confirmed glycan epitope release along the root axes of older plants and the detection of the LM25 xyloglucan and the LM27 heteroxylan epitopes released from larger wheat root systems are shown in Fig. 5.

Detection of root exudate glycan epitopes on root hairs and at the surface of soil particles of rhizosheaths

Short sections of wheat roots with enclosing rhizosheaths (Supplemental Fig. 1) were excised and fixed and whole mount immunofluorescence procedures used to detect epitopes at root hair and soil particle surfaces. The indirect immunolabelling procedures required repeated washing of the samples through which soil particles remained firmly adhered to root hairs/roots (Fig. 6). Signals for the major epitopes contained within wheat HMW exudates were abundant on root hairs (Fig. 6). Root hairs were seen to be clearly attached to the surface of soil particles as revealed by bright field micrographs and the staining of cell walls with Calcofluor White. Fig. 6 shows an example of such micrographs paired with a LM11 xylan micrograph that indicates the detection of the LM11 epitope at regions of root hairs and soil particle surfaces external to root hair cell walls. In some cases extracellular material was clearly visible at root hair and soil particle surfaces and this was strongly bound by the MAbs as shown for LM11. We propose that these observations indicate the presence of wheat root exudate polysaccharides at these locations and that they are key factors in root rhizosheath formation and stabilization.

DISCUSSION

Cereal roots release structurally complex polysaccharides, distinct from cell wall polysaccharides

This analysis of polysaccharides released from wheat and maize roots, and collected in a hydroponic system, indicate a wide range of structural linkages in comparison to cell walls. The same set of monosaccharides was found in exudate polysaccharides as observed in cell walls although there was a very low detection of unidentified hexose and heptose (Table 1). Linkage analysis indicated structural features common in cell wall polysaccharides, however, wheat and maize HMW root exudates display a much wider diversity in the number of linkages in comparison to those seen in, for example, wheat root cell walls (Zabotin et al. 1998) or Arabidopsis cell walls (Pettolino et al. 2012). The diversity of linkages observed in hydroponates is also greater than that seen in previous analyses of wheat and maize root tip mucilage (Bacic et al. 1986; Moody et al. 1988). Previously unreported features include the high proportion of terminal residues indicative of abundant short side branches and considerable diversities of mannosyl, galactosyl and glucosyl linkages. A highly complex polysaccharide with previously unknown structural

features has been reported from a maize aerial root mucilage that harbours nitrogen-fixing bacteria (Amicucci et al. 2019). In contrast to short time period sample collection from root tips, we isolated material released from roots grown over two-week periods in hydroponic systems. This enabled collection of material released from regions in addition to root tips – including the mature root axes and root hairs.

The exudate glycans do contain xylan and xyloglucan epitopes and sandwich-ELISAs indicate that for the wheat samples in particular that they may contain multi-polysaccharide complexes. This is aligned with the increasing recognition and identification of links between cell wall polysaccharide domains (Franková and Fry 2013; Cornuault et al. 2018). For example, the ARABINOXYLAN PECTIN ARABINOGALACTAN PROTEIN1 (APAP1) multidomain polysaccharide identified from the medium of Arabidopsis cell cultures has an AGP and heteroxylan domain along with pectin where AGP forms a core linking the other domains (Tan et al. 2013). The root exudates contain AGP glycan epitopes and it is possible that an AGP may be an organizing factor in their structures. The non-templated synthesis of multi-domain polysaccharides is likely to result in a high heterogeneity of polymers and potential for wide variations in precise structures and indeed properties. The presence of large multi-domain glyco-macromolecules at root surfaces and in rhizospheres may provide potential for modulations in structures between species and within a species dependent upon growth conditions. Indeed, analysis of potato root exudates has provided evidence that some AGP components of exudates increased in response to a bacterial pathogen (Koroney et al. 2016).

The function of the structural complexity of exudate polysaccharides is far from clear but may relate to the putative soil-binding properties – work with model polysaccharides has indicated strong binding properties for both glucans and highly branched polysaccharides (Akhtar et al. 2018). Future work will be required to determine the macromolecular compositions of the exudates and the possible presence of strong soil-binding sub-fractions. The structural complexity of exudate polysaccharides may also relate to their role as substrates for microbiota in soils and different polysaccharides are likely to influence microbe population dynamics in different ways. Related to this, exudate structural complexity may act to provide some recalcitrance to microbial degradation.

Available glycan MAbs provide molecular tools to track exudate polysaccharides but not a full coverage of exudate polysaccharide structural features

Using sets of antibodies directed to cell walls, we have identified epitopes for heteroxylan, xyloglucan and glycoproteins in the root HMW exudates. The detection of these epitopes confirms the presence of these polymers as indicated by the monosaccharide linkage analyses. However, there clearly is potential for development of probes directed to previously undocumented features of root exudates that would allow for specific tracking of exudate components in terms of biosynthesis and cellular exudation processes. However, the current availability of MAbs that bind to the HMW exudates, most notably the structurally defined LM11 xylan, LM25 xyloglucan and LM2 AGP epitopes has enabled the initial tracking of exudates. Analysis of these epitopes indicates that the exudates are released along root axes and are associated with root hairs in rhizosheaths. This observation indicates the potential for distinct secretions from root axes and root apices. It is of interest here that the LM8 xylogalacturonan epitope, associated with cell detachment including root caps across species (Willats et al. 2004), was not detected in the exudate samples or at root hairs in rhizosheath soils (Fig. 6). This likely relates to the restriction of this epitope to the root tip as a component of less soluble mucilage.

HMW glycan exudates, soil-binding factors, rhizosheaths and the rhizosphere

Rhizosheaths have been a focus for much recent work and consideration of their potential to be important factors associated with enhanced nutrient and water uptake and are a potential breeding target particularly for water-limited grain crops (Adu et al. 2017; Brown et al. 2017; Rabbi et al. 2018; Young and Bengough 2018; York et al. 2016; George et al. 2014). Understanding the mechanistic basis of their formation and stabilization is therefore of broad economic and social interest. Adhesive mucilage is recognised as an important component of rhizosheaths (Ahmed et al. 2018; Rabbi et al. 2018). Root hair length of the same genotype can vary between soil conditions and can influence rhizosheath mass (Haling et al. 2014) and there is clearly potential for adhesive secretions to contribute to this. Additional proposed roles for polysaccharide-rich mucilage include facilitating the diffusion of low molecular weight exudates and influencing microbial activity when water is limiting (Holz et al. 2018). The work reported here does not define the adhesive component of HMW exudates in molecular detail but it does outline structural features in adhesive exudates and evidence for these being associated with root hairs entangled with rhizosheath soil particles. Work will be required to dissect the exudates further and track

their fate in soils. Polysaccharides are well established substrates for microbial metabolism and the features of HMW exudates, if they indeed are responsive to growth conditions, may influence subsets of microbiota as indicated for small molecular weight compounds (Dennis et al. 2010; Zhalnina et al. 2018).

How exudates, collected from hydroponic systems without the mechanical stimulus and support of soils, relate to those when plant grow in soils and rhizosheaths form, are not known in detail although this work confirms the presence of common polysaccharide epitopes. The isolation of adhesive molecules from rhizosheath soils and the root hair-soil interface and their analysis remains technically challenging with most studies collecting mucilage from exposed root tips (York et al. 2016; Oburger and Jones 2018). Indeed, studies in maize have shown that root hairs are more abundant and mucilage more adhesive in drier soils (Watt et al. 1994) indicative of some flexibility in mucilage structures discussed above. It will be of interest to understand any differential capacity of soil-binding polysaccharides/polysaccharide complexes in relation to the chemistry of soil particles, the extent and nature of soil organic matter and even other aspects of soils such as pH and water content.

In summary, we have extended knowledge of the HMW glycans released from cereal roots and developed methodologies for future studies to refine their roles in rhizosheath formation and stability. Knowledge of polysaccharide exudate chemistry and associated molecular tools will be useful for the screening of genetic populations and the identification of underground traits of relevance to crop breeding.

MATERIALS & METHODS

Plant material and hydroponic and growth systems

Wheat (*Triticum aestivum* L. cv. Cadenza) and maize (*Zea mays* L. F1 'Earlibird') seeds were germinated and grown in vermiculite and perlite (50:50) for 7 days with a photoperiod of 12 h at 22°C and photosynthetic photon flux density (PPFD) of 634 µmol m^{-1} s^{-1}. Plants were then transferred to a hydroponic system in which 12 plants were grown in 9 L of half-strength Hoagland nutrient solution with a constant air flow through the medium for 14 days in a glasshouse at 22°C, 16 h photoperiod and 1,382 µmol m^{-1} s^{-1} PPFD as described (Galloway et al. 2018). Hydroponates were collected, passed through Whatman grade 114V filter paper and then high molecular weight (HMW) material isolated by concentration of 9 L volumes to ~200 mL (using a Centramate Ultrafiltration system with

30,000 Da cut-off membrane (PALL, US)) and dialysis against water and freeze-dried as described (Galloway et al. 2018).

For nitrocellulose-based immunolabelling of polysaccharides released by young seedlings wheat grain were germinated on sterile moist filter paper in 10 cm x 10 cm plastic dishes prior to transfer to nitrocellulose sheets for 2 h. In some cases, the seedlings on filter paper were flooded in situ with 40 ml 8% (v/v) formaldehyde in water overnight prior to transfer to nitrocellulose sheets. Non-fixed seedlings were flooded with an equivalent volume of water. For the immunodetection of epitopes released by larger root systems of hydroponically grown plants the root systems were laid on nitrocellulose sheets for 10 min prior to removal and processing. For the immunolabelling of whole roots/rhizosheaths plants were grown in a 50:50 mixture of a sandy loam topsoil and sand for 14 days within a glasshouse.

Carbohydrate composition and monosaccharide linkage analysis.

Carbohydrate monosaccharide linkage analyses of the wheat and maize root HMW exudate polysaccharides were performed by the analytical services of the Complex Carbohydrate Research Center, Georgia (US). For glycosyl linkage analysis, the samples were carboxyl methylated, reduced, permethylated again, reduced, hydrolyzed and acetylated; and the resultant partially methylated alditol acetates (PMAAs) analyzed by gas chromatography-mass spectrometry (GC-MS). In detail, ~1 mg of each sample was treated with 0.5 M methanolic HCl for 20 min at 80°C. The samples were then dried, and reduction of the carboxylic acids was accomplished using 400 µl of a 10 mg/ml solution NaBD4 in water overnight. The samples were then neutralized with acetic acid and dried thoroughly. The dried samples were then suspended in 200 µl of dimethyl sulfoxide. Permethylation of the sample was achieved by two rounds of treatment with sodium hydroxide (15 min) and methyl iodide (45 min). The permethylated sample carboxylic acids were reduced by adding 200 µl of a 5 mg/ml solution of LiBD4 in 90% tetrahydrofuran and reacting overnight at RT, followed by 1 h at 100°C. The samples were then hydrolyzed using 0.1 M trifluoroacetic acid (TFA) (0.5 h in sealed tube at 100°C), reduced with NaBD4, hydrolyzed again using 2 M TFA (2 h in sealed tube at 100°C) and acetylated using acetic anhydride/TFA. The resulting PMAAs were analyzed on an Agilent 7890A GC interfaced to a 5975C MSD (mass selective detector, electron impact ionization mode); separation was performed on a 30 m Supelco SP-2331 bonded phase fused silica capillary column.

Soil-binding assays and periodate oxidation

The capacity of root exudates to bind soil was determined using a nitrocellulose-based assay as described (Akhtar et al. 2018). The periodate oxidation treatment to confirm carbohydrate involvement in soil binding was adapted from Woodward et al. 1985. After application HMW materials to nitrocellulose sheets they were dried and then incubated in 25 mM sodium metaperiodate in 50 mM sodium acetate buffer (pH 4.5) for 18 h. Sheets without periodate oxidation treatment were incubated in sodium acetate buffer alone for the same period. Sheets were then washed in dH_2O for 3 x 5 min prior to the addition of soil.

Monoclonal antibodies and carbohydrate-binding modules

The characteristics of the panels of established rat and mouse MAbs, directed to cell wall polysaccharides, used in the study are largely outlined elsewhere (Ruprecht et al. 2017; Cornuault et al. 2018). These included LM1 extensin, LM5 galactan, LM6-M arabinan, LM8 xylogalacturonan, LM10, LM11 & LM28 heteroxylan, LM15 & LM25 xyloglucan, LM19 & JIM7 homogalacturonan, LM21 heteromannan, and LM2, JIM13 & MAC207 AGP along with BS400-2 callose and BS400-3 mixed-linkage glucan. Additional probes included CCRC-M170 acetylated mannan (Zhang et al. 2014), LM26 galactan (Torode et al. 2018), LM27 heteroxylan (Cornuault et al. 2015) and LM4 pea amine oxidase (a non-binding MAb, Laurenzi et al. 2001). Carbohydrate-binding modules (CBMs) used included CBM2b1-2 xylan (McCartney et al. 2006) and CBM27 mannan (Marcus et al. 2010).

ELISAs and nitrocellulose-based antibody analyses

ELISAs were performed with potential antigens incubated overnight in the presence of phosphate-buffered saline (PBS) to promote adhesion to microtitre plates (Nunc Maxisorp, Thermo Scientific, Denmark) as described (Cornuault et al. 2018). All microtitre plates were blocked with 5% (w/v) milk powder/PBS (MP/PBS) prior to probing with antibodies. Sandwich-ELISAs were carried out with microtitre plates pre-coated overnight at 4°C with 10 µg/mL xylan-binding CBM2b1-2 or mannan-binding CBM27 to act as capture probes and as described (Cornuault et al. 2015). After plates were blocked with MP/PBS isolated HMW material from hydroponates at 10 µg/mL in the presence of block was incubated in plate wells overnight at 4°C, washed and then probed by rat antibodies using standard procedures. Seedling prints on nitrocellulose sheets were carried out with rat MAbs at 10-

fold dilution of hybridoma supernatants followed by anti-rat IgG horseradish peroxidase and a chloronaphthol-based substrate as previously described (Galloway et al. 2018).

Whole mount immunolabelling of rhizosheaths

A whole mount approach was taken for the *in situ* immunoanalysis of samples of wheat roots with attached rhizosheaths. No water was provided to growing wheat plants for three days prior to analysis to promote isolation of rhizosheaths and samples were collected by gently excavating the roots from the soil-sand mix. Small sections (~1 cm) of root with soil attached were cut and fixed in 4% (v/v) formaldehyde PEM buffer (50 mM PIPES, 5 mM EGTA, 5 mM MgSO4, pH 6.9) overnight. The materials were then blocked in MP/PBS for 30 min, washed and incubated with rat MAbs at 5-fold dilution in MP/PBS for at least 90 min. After washing with PBS materials were incubated with anti-rat FITC (Sigma-Aldrich, US) at 100-fold dilution for at least 90 min. After washing the samples were incubated with Calcofluor White (0.2 µg/mL) (Fluorescent Brightner 28, Sigma-Aldrich, UK) washed in PBS and then mounted in a glycerol-based antifade solution (Citifluor AF1, Agar Scientific, UK). Immunofluorescence was observed with a microscope equipped with epifluorescence irradiation (Olympus BX-61) and micrographs captured with a Hamamatsu ORCA285 camera and with Perkin-Elmer Volocity software. All images/micrographs shown are representative of at least four separate experiments with each MAb.

DATA AVAILABILITY

All relevant data can be found within the manuscript and its supporting materials.

ACKNOWLEDGMENTS. The authors acknowledge the award of a University of Leeds Anniversary Research Scholarship to AFG and also support from the UK Biotechnology & Biological Sciences Research Council (BBSRC) (PK, BB/K017489/10). JA was supported by a BBSRC DTP grant (BB/M011151/1). KJF was supported by a BBSRC Translational Fellowship (BB/M026825/1). This work was also supported by the Chemical Sciences, Geosciences and Biosciences Division, Office of Basic Energy Sciences, U.S. Department of Energy grant (DE-SC0015662) to Parastoo Azadi at the Complex Carbohydrate Research Center.

AUTHOR CONTRIBUTIONS

AFG and JA prepared and analysed the hydroponates, JA, SEM, NF and PK carried out root printing, soil growth and microscopy experiments. KF and PK supervised the experiments. PK wrote the manuscript with contributions from all authors and all authors read and approved the final manuscript.

CONFLICTS OF INTEREST

The authors declare that they have no competing interests.

SUPPORTING INFORMATION

Additional Supporting Information may be found in the online version of this article.

Figure S1. Rhizosheaths at the surface of wheat and maize roots.

REFERENCES

Adu, M.O., Asare, P.A., Yawson, D.O, Ackah, F.K., Amoah, K.K., Nyarko, M.A., and Andoh, D.A. (2017) Quantifying variations in rhizosheath and root system phenotypes of landraces and improved varieties of juvenile maize. *Rhizosphere,* **3**, 29-39.

Ahmed MA, Passioura J, and Carminati A (2018) Hydraulic processes in roots and the rhizosphere pertinent to increasing yield of water-limited grain crops: a critical review. *J. Exp. Bot*. **69**, 3255-3265.

Akhtar, J., Galloway, A.F., Nikolopoulos, G., Field, K.J., and Knox, P. (2018) A quantitative method for the high throughput screening for the soil adhesion properties of plant and microbial polysaccharides and exudates. *Plant & Soil*, **428**, 57-65.

Amicucci, M.J., Galermo, A.G., Gurrrero, A., Treves, G., Nandita, E., Kailemia, M.J., Higdon, S.M., Pozzo, T., Labavitch, J.M., Bennett, A.B., and Lebrilla, C.B. (2019) Strategy for structural elucidation of polysaccharides: elucidation of a maize mucilage that harbors diazotrophic bacteria. *Anal. Chem.* **91**, 7254-7265.

Bacic, A., Moody, S.F., and Clarke, A.E. (1986) Structural analysis of secreted root slime from maize (*Zea mays* L.). *Plant Physiol.* **80**, 771-777.

Benard, P., Zarebanadkouki M., Brax, M., Kaltenbach, R., Jerjen, I., Marone, F., Couradeau, E., Felde, V.J.M.N.L., Kaestner A., and Carminati, A. (2019) Microhydrological niches in soils: How mucilage and EPS alter the biophysical properties of the rhizosphere and other biological hotspots. *Vadose Zone J.* 18, 180211.

Brown, L.K., George, T.S., Neugebauer, K., and White, P.J. (2017) The rhizosheath – a potential trait for future agricultural sustainability occurs in orders throughout the angiosperms. *Plant & Soil,* **418**, 115-128.

Chaboud, A., and Rougier, M. (1990) Comparison of maize root mucilages isolated from root exudates and root surface extracts by complementary cytological and biochemical investigations. *Protoplasma*, **156**, 163-173.

Cornuault, V., Buffetto, F., Rydahl, M.G., Marcus, S.E., Torode, T.A., Xue, J., Crépeau, M., Faria-Blanc, N., Willats, W.G.T., Dupree, P., Ralet, M. and Knox, J.P. (2015) Monoclonal antibodies indicate low-abundance links between heteroxylan and other glycans of plant cell walls. *Planta,* **242**, 1321-1334.

Cornuault, V., Posé, S. and Knox, J.P. (2018) Disentangling pectic homogalacturonan and rhamnogalacturonan-I polysaccharides: evidence for sub-populations in fruit parenchyma systems. *Food Chem.* **246**, 275-285.

Delhaize, E., Rathjen, T.M. and Cavanagh, C.R. (2015) The genetics of rhizosheath size in a multiparent mapping population of wheat. *J. Exp. Bot.* **66**, 4527-4536.

Dennis, P.G., Miller, A,J. and Hirsch, P.R. (2010) Are root exudates more important than other sources of rhizodeposits in structuring rhizosphere bacterial communities? *FEMS Microbiol. Ecol.* **72**, 313-327.

Franková, L. and Fry, S.C. (2013) Biochemistry and physiological roles of enzymes that 'cut and paste' plant cell-wall polysaccharides. *J. Exp. Bot.* **64**, 3519-3550.

Galloway, A.F., Pedersen, M.J., Merry, B., Marcus, S.E., Blacker, J., Benning, L.G., Field, K.J. and Knox, J.P. (2018) Xyloglucan is released by plants and promotes soil particle aggregation. *New Phytol.* **217**, 1128-1136.

George, T.S., Brown, L.K., White, P.J., Newton, A.C., Bengough, A.G., Russell, J. and Thomas, W.T.B. (2014) Understanding the genetic control and physiological traits associated with rhizosheath production by barley *(Hordeum vulgare*). New Phytol. **203**, 195-205.

Guinel, F.C. and McCully, M.E. (1986) Some water-related physical properties of maize root-cap mucilage. *Plant Cell Environ.* **9**, 657-666.

Haling, R.E., Brown, L.K., Bengough, A.G., Valentine, T.A., White, P.J., Young, I.M. and George, T.S. (2014) Root hair length and rhizosheath mass depend on soil porosity, strength and water content in barley genotypes. *Planta*, **239**, 643-651.

Holz, M., Zarebanadkouki, M., Kaestner, A., Kuzyakov, Y. and Carminati, A. (2018) Rhizodeposition under drought is controlled by root growth rate and rhizosphere water content. *Plant & Soil*, **423**, 429-442.

Knee, E.M., Gong, F.-C., Gao, M., Teplitski, M., Jones, A.R., Foxworthy, A., Mort, A.J. and Bauer W.D. (2001) Root mucilage from pea and its utilization by rhizosphere bacteria as a sole carbon source. *Mol Plant Microbe Int.* **14**, 775-784.

Koroney A.S., Plasson, C., Pawlak, B., Sidikou, R., Driouich, A., Menu-Bouaouiche, L. and Vicre-Gibouin, M. (2016) Root exudate of Solanum tuberosum is enriched in galactose-containing molecules and impacts the growth of *Pectobacterium atrosepticum. Ann Bot.* **118**, 797-808.

Laurenzi, M., Tipping, A.J., Marcus, S.E., Knox, J.P., Federico, R., Angelini, R. and McPherson, M.J. (2001) Analysis of the distribution of copper amine oxidase in cell walls of legume seedlings. *Planta* **214**, 37-45.

Liu, T-Y., Ye, N., Song, T., Cao, C., Gao, Y., Zhang, D., Zhu, F., Chen, M., Zhang, Y., Xu, W., and Zhang, J. (2019) Rhizosheath formation and involvement in foxtail millet (*Setaria italic*) root growth under drought stress. *J. Integrative Plant Biol.* **61**, 449-462.

Moody, S.F., Clarke, A.E. and Bacic, A. (1988) Structural analysis of secreted slime from wheat and cowpea roots. *Phytochem*. **27**, 2857-2861.

McCartney, L., Blake, A.W., Flint, J., Bolam, D.N., Boraston, A.B., Gilbert, H.J. and Knox, J.P. (2006) Differential recognition of plant cell walls by microbial xylan-specific carbohydrate-binding modules. *Proc Nat Acad Sci USA* **103**, 4765-4770.

Marcus, S.E., Blake, W.A., Benians, T.A., Lee, K.J.D., Poyser, C., Donaldson, I., Leroux, O., Rogowski, A., Petersen, H.L., Boraston, A., Gilbert, H.J., Willats, W.G.T. and Knox J.P. (2010) Restricted access of proteins to mannan polysaccharides in intact plant cell walls. *Plant J.* **64**, 191-203.

Naveed, M., Brown, L.K., Raffan, A.C., George, T.S., Benough, A.G., Roose, T., Sinclair, I., Koebernick, N., Coooper, L., Hackett, C.A. and Hallett P.D. (2017) Plant exudates may stabilise or weaken soil depending on species, origin and time. *Eur J Soil Sci.* **68**, 806-816.

Oburger, E. and Jones, D.L. (2018) Sampling root exudates – mission impossible. *Rhizosphere*, **6**, 116-133.

Pang, J., Ryan, M.H., Siddique, K.H.M., and Simpson, R.J. (2017) Unwrapping the rhizosheath. *Plant & Soil*, **418**, 129-139.

Pettolino, F.A., Walsh, C., Fincher, G.B. and Bacic A. (2012) Determining the polysaccharide composition of plant cell walls. *Nature Protocols* **7**, 1590-1607.

Rabbi S.M.F., Tighe M.K., Flavel R.J., Kaiser B.N., Guppy C.N., Zhang X. and Young I.M. (2018) Plant roots redesign the rhizosphere to alter the three-dimensional physical architecture and water dynamics. *New Phytol.* **219**, 542-550.

Ruprecht, C., Bartetzko, M.P., Senf, D., Dallabernardina, P., Boos, I., Andersen, M.C.F., Kotake, T., Knox, J.P., Hahn, M.G., Clausen, M.H. and Pfrengle, F. (2017) A synthetic glycan microarray enables epitope mapping of plant cell wall glycan-directed antibodies. *Plant Physiol.* **175**, 1094-1104.

Tan, I., Eberhard, S., Pattathil, S., Warder, C., Glushka, J., Yuan, C., Hao, Z., Zhu, X., Avci, U., Miller, J.S., Baldwin, D., Pham, C., Orlando, R., Darvill, A., Hahn, M.G., Kieliszewski, M.J. and Mohnen, D. (2013) An Arabidopsis cell wall proteoglycan consists of pectin and arabinoxylan covalently linked to an arabinogalactan protein. *Plant Cell,* **25**, 270-287.

Torode, T.A., O'Neill, R., Marcus, S.E., Cornuault, V., Posé, S., Lauder, R.P., Kračun, S.K., Rydahl, M.G., Andersen, M.C.F., Willats, W.G.T., Braybrook, S.A., Townsend, B.J., Clausen, M.H., and Knox, J.P. (2018) Branched pectic galactan in phloem-sieve-element cell walls: implications for cell mechanics. *Plant Physiol.* **176**, 1547-1558.

Tisdall, J.M., and Oades, J.M. (1982) Organic matter and water stable aggregates in soils. *J. Soil Sci.* **3**, 141-167.

Walker, W.S., Bais, H.P., Grotewold, E., and Vivanco, J.M. (2003) Root exudation and rhizosphere biology. *Plant Physiol.* **132,** 44-51.

Watt, M., McCully, M.E., and Canny, M.J. (1994) Formation and stabilization of rhizosheaths of *Zea mays* L. Effect of soil water content. *Plant Physiol.* **106**, 179-186.

Watt, M., McCully, M.E., and Jeffree, C.E. (1993) Plant and bacterial mucilages of the maize rhizosphere: comparison of their soil binding-properties and histochemistry in a model system. *Plant and Soil* 151, 151-165.

Willats, W.G.T., McCartney, L., Steele-King, C.G., Marcus, S.E., Mort, A., Huisman, M., van Alebeek, G.-J., Schols, H.A., Voragen, A.G.J., Le Goff, A., Bonnin, E., Thibault, J.-F. and Knox, J.P. (2004) A xylogalacturonan epitope is specifically associated with plant cell detachment. *Planta*, **218**, 673-681.

Woodward, M.P., Young Jr., W.W., and Bloodgood, R.A. (1985) Detection of monoclonal nntibodies specific for carbohydrate epitopes using periodate oxidation. *J. Immunol. Methods*, **78**, 143-153.

Young, I.M. and Bengough, A.G. (2018) The search for the meaning of life in soil: an opinion. *Eur J. Soil Sci.* **69**, 31-38.

York, L.M., Carminati, A., Mooney, S.J., Ritz, K. and Bennett, M.J. (2016) The holistic rhizosphere: integrating zones, processes, and semantics in the soil influenced by roots. *J. Exp Bot.* **67**, 3629-3643.

Zabotin, A.I., Barisheva, T.S., Zabotina, O.A., Larskaya, I.A., Lozovaya, V.V., Beldman, G. and Voragen, A.G.J. (1998) Alterations in cell walls of winter wheat roots during low temperature acclimation. *J. Plant Physiol.* **152**, 473-479.

Zhalnina, K., Louie, K.B., Hao, Z., Mansoori, N., Nunes da Roch,a U., Shi, S., Cho, H., Karaoz, U., Loqué, D., Bowen, B.P., Firestone, M.K., Northen, T.R. and Brodie E.L. (2018) Dynamic root exudate chemistry and microbial substrate preferences drive patterns in rhizosphere microbial community assembly. *Nature Microbiol.* **3**, 470–480.

Zhang, X., Rogowski, A., Zhao, L., Hahn, M.G., Avci, U., Knox, J.P. and Gilbert H.J. (2014) Understanding how the complex molecular architecture of mannan degrading hydrolases contributes to plant cell wall degradation. *J. Biol. Chem.* **289**, 2002-2012.

FIGURE LEGENDS

Figure 1. The soil-binding properties of HMW compounds of root exudates are sensitive to periodate oxidation treatment. A. Representative examples of nitrocellulose sheets loaded with 5 µl spots of 50 µg and 10 µg HMW compounds from wheat and maize. B. Quantification of bound soil for 50 µg spots, n = 6, error bars = SD. Significant differences between treatments denoted: *** P <0.001.

Figure 2. Heatmap of glycan epitope detection in HMW exudates from wheat and maize samples for which the monosaccharide linkage analysis is shown in Table 1. ELISA absorbance (Abs) values shown for HMW exudates at 10 µg/ml are means of 3 replicates with SD. Significant differences between species means denoted: * P <0.05. Scale for conditional formatting (green) of absorbance values shown to right. AGP = arabinogalactan-protein, HG = homogalacturonan, MLG = mixed-linkage glucan, XG, xylogalacturonan, BS = BioSupplies antibody.

Figure 3. Sandwich-ELISA analysis of links between major glycan epitopes found in HMW exudates. CBMs used as capture molecules and MAbs as detection molecules. Means of absorbance shown with SD, n = 6. Significant differences between CBMs denoted * P <0.01. Use of xylan-binding CBM2b1-2 as capture molecule and incubation of HMW exudates leads to capture of xyloglucan (LM25) and AGP (LM2) epitopes in wheat samples. Use of mannan-binding CBM27 does not lead to capture of HMW exudate epitopes.

Figure 4. Wheat seedlings release glycan epitopes present in HMW exudates and soil-binding factors along the root axis. Top paired panels show wheat seedlings that were placed on nitrocellulose sheets for 2 h and associated probing of sheets with LM25 xyloglucan, LM11 xylan and LM2 AGP MAbs after seedling removal. Middle panels show the absence of binding of irrelevant MAb LM4 and the loss of LM11 signal after pre-fixation of seedling. Bottom paired panels show a seedling and corresponding nitrocellulose sheet processed for the soil adhesion procedure (Akhtar et al. 2018). Arrows indicate root regions that released strong soil-binding molecules. Arrowheads indicate soil adhered at root tip positions. All nitrocellulose sheet images shown are representative of at least three replicates. Scale bars = 10 mm.

Figure 5. Imaging of glycan epitopes in HMW exudates released from large wheat roots grown hydroponically for 2 weeks and then lain on sheets of nitrocellulose for 10 min prior to probing with MAbs. Images of root systems shown for the LM25 xyloglucan and the LM27 heteroxylan epitopes. All images scaled to the same extent and bar = 100 mm.

Figure 6. Immunofluorescence detection in whole mount preparations of glycan epitopes on wheat root hairs in rhizosheaths. Top row: Paired bright field (BF) and LM25 xyloglucan immunofluorescence micrographs of the same region of rhizosheath soil attached to a wheat root. Bar = 500 µm. Middle row: Comparative immunofluorescence micrographs with LM2 AGP and LM8 xylogalacturonan (non-binding) MAbs. Bars = 1 mm. Bottom row: Micrographs of soil particles attached to root hairs showing BF, Calcofluor White (CW) staining of cell walls and LM11 xylan epitope detection. Arrow heads indicate epitope detection on soil particle surfaces that are not part of cellulosic root hair cell walls. Bar = 200 µm.

Table 1. Monosaccharide linkage analysis of wheat and maize hydroponates samples. Linkages shown as Mol%. Combined data (n =4) showing means and SD from hydroponates grown on two separate occasions. Column headed with * indicates significantly different means between the two species (* P <0.05, ** P <0.01, *t*-test). Final column indicates for some linkages possible polysaccharide/glycoprotein classes the residues arise from (Pettolino et al. 2012). AGP - arabinogalactan-protein, C – cellulose, CA – callose, E – extension, HG – homogalacturonan, HM – heteromannan, HX – heteroxylan, MLG – mixed-linkage glucan, RGI – rhamnogalacturonan-I, XG – xyloglucan.

Monosaccharide	Linkage	**Wheat**		**Maize**		*	Polysaccharide
		Mean	**SD**	**Mean**	**SD**		
Arap	Terminal	4.5	1.9	2.6	0.4		AGP
	2-	0.3	0.3	0.1	0.1		
	3-	0.5	0.5	0.2	0.2		
	4-	1.7	1.5	1.4	1.0		
Araf	Terminal	2.6	0.9	1.2	0.4	*	AGP, HX, RGI
	2-	0.2	0.1	0.0	0.0	*	AGP, E, HX
	3-	0.3	0.4	0.5	0.5		E
Arabinose	**Total**	**9.9**	4.0	**5.9**	1.7		
Fuc	Terminal	1.1	0.7	4.6	1.8	*	XG
	3-	0.3	0.3	0.3	0.4		
	3,4-	0.3	0.3	0.4	0.4		
Fucose	**Total**	**1.6**	0.9	**5.3**	1.9	*	
Galp	Terminal	10.2	2.7	19.8	2.7	**	AGP, RGI, XG
	2-	0.1	0.1	0.2	0.2		
	3-	1.6	0.9	1.7	0.5		AGP
	4-	0.7	0.3	1.3	0.6		RGI
	6-	1.1	0.8	2.2	1.0		AGP
	2,3-	0.1	0.1	0.1	0.1		
	2,4-	0.2	0.2	0.1	0.1		
	3,4-	0.1	0.2	0.3	0.2		
	3,6-	0.2	0.2	0.4	0.2		AGP
	4,6-	0.2	0.2	0.4	0.4		RGI
	3,4,6-	0.0	0.0	0.1	0.1		
Galf	Terminal	2.1	0.7	3.6	1.3		
Galactose	**Total**	**16.4**	4.7	**30.0**	4.4	**	
Glc	Terminal	9.1	2.0	8.5	1.1		
	2-	1.2	0.4	1.2	0.4		
	3-	2.4	1.6	2.2	1.1		CA
	4-	12.2	3.4	7.3	3.3		C, HM,MLG, XG
	6-	1.5	0.6	1.7	0.8		
	2,3-	0.1	0.1	0.1	0.1		
	2,4-	0.3	0.3	0.2	0.2		
	3,4-	0.4	0.4	0.5	0.6		

	3,6-	0.4	0.3	0.4	0.5		
	4,6-	7.6	3.1	3.9	2.9		XG
	2,4,6-	0.2	0.2	0.0	0.0		
	3,4,6-	0.3	0.0	0.0	0.0		
Glucose	**Total**	**35.4**	6.2	**25.8**	3.2		
Xyl	Terminal	7.4	1.9	3.6	0.7	*	XG
	2-	0.4	0.2	0.5	0.1		XG
	4-	1.9	1.0	1.6	0.4		HX
Xylose	**Total**	**9.6**	1.5	**5.6**	1.0	**	
Rha	Terminal	3.8	0.7	2.7	1.0		AGP
	2-	0.3	0.1	0.5	0.1		
	3,4-	0.4	0.3	0.2	0.2		
Rhamnose	**Total**	**4.4**	0.8	**3.3**	1.0		
GlcA	Terminal	3.0	1.3	3.3	0.8		AGP, HX
	4-	3.1	1.6	1.6	1.4		
	3,4-(4,6-)	0.8	0.0	0.4	0.3		
Glucuronic Acid	**Total**	**5.5**	1.8	**5.3**	1.2		
GalA	4-	0.2	0.1	0.2	0.1		
Galacturonic Acid	**Total**	**0.2**	0.1	**0.2**	0.1		
Man	Terminal	6.8	1.1	6.4	1.1		
	2-	2.9	0.7	5.1	0.9	*	
	3-	1.4	0.8	1.1	0.4		
	4-	2.1	1.0	1.6	1.0		HM
	6-	0.4	0.3	0.5	0.1		
	2,3-	1.4	0.6	2.5	1.1		
	2,4-	0.1	0.1	0.2	0.2		
	2,6-	0.0	0.0	0.4	0.4		
	3,4-	0.1	0.1	0.2	0.3		
	3,6-	0.2	0.2	0.1	0.1		
	4,6-	1.7	1.2	0.3	0.1		HM
	2,3,6-	0.0	0.0	0.1	0.1		
	2,4,6-	0.1	0.1	0.1	0.1		
	3,4,6-	0.1	0.1	0.1	0.1		
Mannose	**Total**	**17.2**	1.5	**17.8**	4.1		
Hexf	2-	0.0	0.0	0.1	0.1		
Hexose	**Total**	0.0	0.0	0.1	0.1		
Hep	Terminal	0.3	0.4	0.3	0.3		
	2-	0.3	0.6	0.0	0.0		
Heptose	**Total**	0.6	0.6	0.3	0.3		
ALL TOTAL		100.6		99.5			

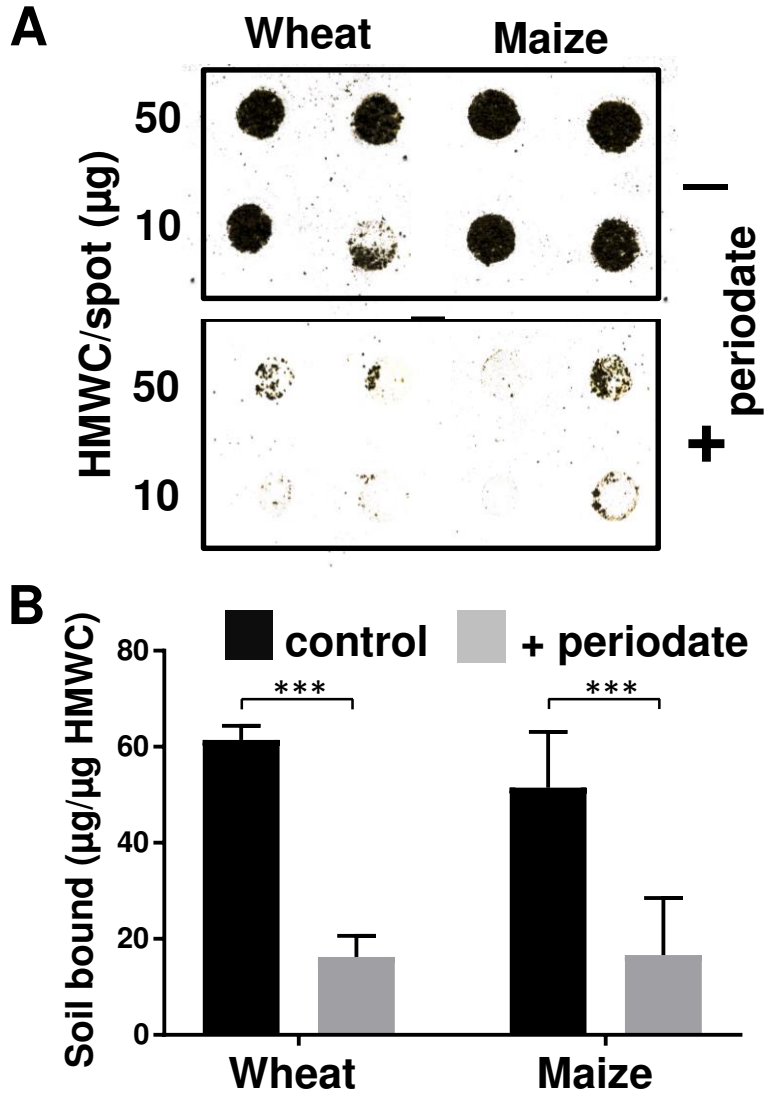

Fig. 1. The soil-binding properties of HMW compounds of root exudates are sensitive to periodate oxidation treatment. A. Representative examples of nitrocellulose sheets loaded with 5 µl spots of 50 µg and 10 µg HMW compounds of root exudates from wheat and maize. B. Quantification of bound soil for 50 µg spots, n = 6, error bars = SD. Significant differences between treatments denoted: *** P <0.001.

Glycan	MAb	Wheat Mean	Wheat SD	Maize Mean	Maize SD	*
Heteroxylan	**LM10**	0.40	0.09	0.04	0.04	*
	LM11	1.25	0.23	0.92	0.31	
	LM27	1.76	0.13	1.42	0.59	
	LM28	0.17	0.09	0.21	0.06	
Xyloglucan	**LM15**	0.33	0.26	0.00	0.00	*
	LM25	1.83	0.01	1.08	0.22	*
AGP	**LM2**	0.55	0.21	0.22	0.09	
	LM30	0.00	0.00	0.00	0.00	
	JIM13	0.16	0.09	0.01	0.01	*
	MAC207	0.06	0.05	0.04	0.00	
Extensin	**LM1**	0.49	0.16	0.03	0.02	*
Pectic HG	**LM19**	0.13	0.10	0.02	0.01	
	JIM7	0.00	0.00	0.00	0.00	
Pectic XG	**LM8**	0.00	0.00	0.00	0.00	
Pectic galactan	**LM5**	0.00	0.00	0.00	0.01	
	LM26	0.00	0.00	0.00	0.00	
Pectic arabinan	**LM6-M**	0.00	0.00	0.00	0.00	
Heteromannan	**LM21**	0.00	0.00	0.00	0.00	
	CCRC-M170	0.00	0.00	0.00	0.00	
	CBM27	0.00	0.00	0.00	0.00	
β-glucan	**BS:1,3-glucan**	0.00	0.00	0.00	0.00	
	BS:1,3-1,4-glucan	0.00	0.00	0.00	0.00	

Abs Scale
2.0
1.5
1.0
0.5
0.0

Fig. 2. Heatmap of glycan epitope detection in HMW exudates from wheat and maize samples for which the monosaccharide linkage analysis is shown in Table 1. ELISA absorbance (Abs) values shown for HMW exudates at 10 µg/ml are means of 3 replicates with SD. Significant differences between species means denoted: * P <0.05. Scale for conditional formatting (green) of absorbance values shown to right. AGP = arabinogalactan-protein, HG = homogalacturonan, MLG = mixed-linkage glucan, XG, xylogalacturonan, BS = BioSupplies antibody.

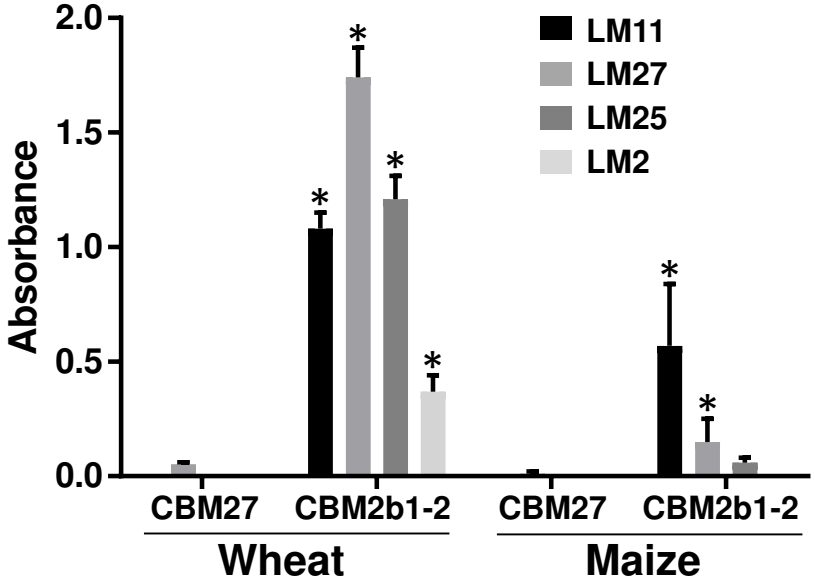

Fig. 3. Sandwich-ELISA analysis of links between major glycan epitopes found in HMW exudates. CBMs used as capture molecules and MAbs as detection molecules. Means of absorbance shown with SD, n = 6. Significant differences between CBM27 and CBM2b1-2 denoted * ($P < 0.01$) above CBM2b1-2 values. Use of xylan-binding CBM2b1-2 as capture molecule and incubation of HMW exudates leads to capture of xyloglucan (LM25) and AGP (LM2) epitopes in wheat samples. Use of mannan-binding CBM27 does not lead to capture of HMW exudate epitopes.

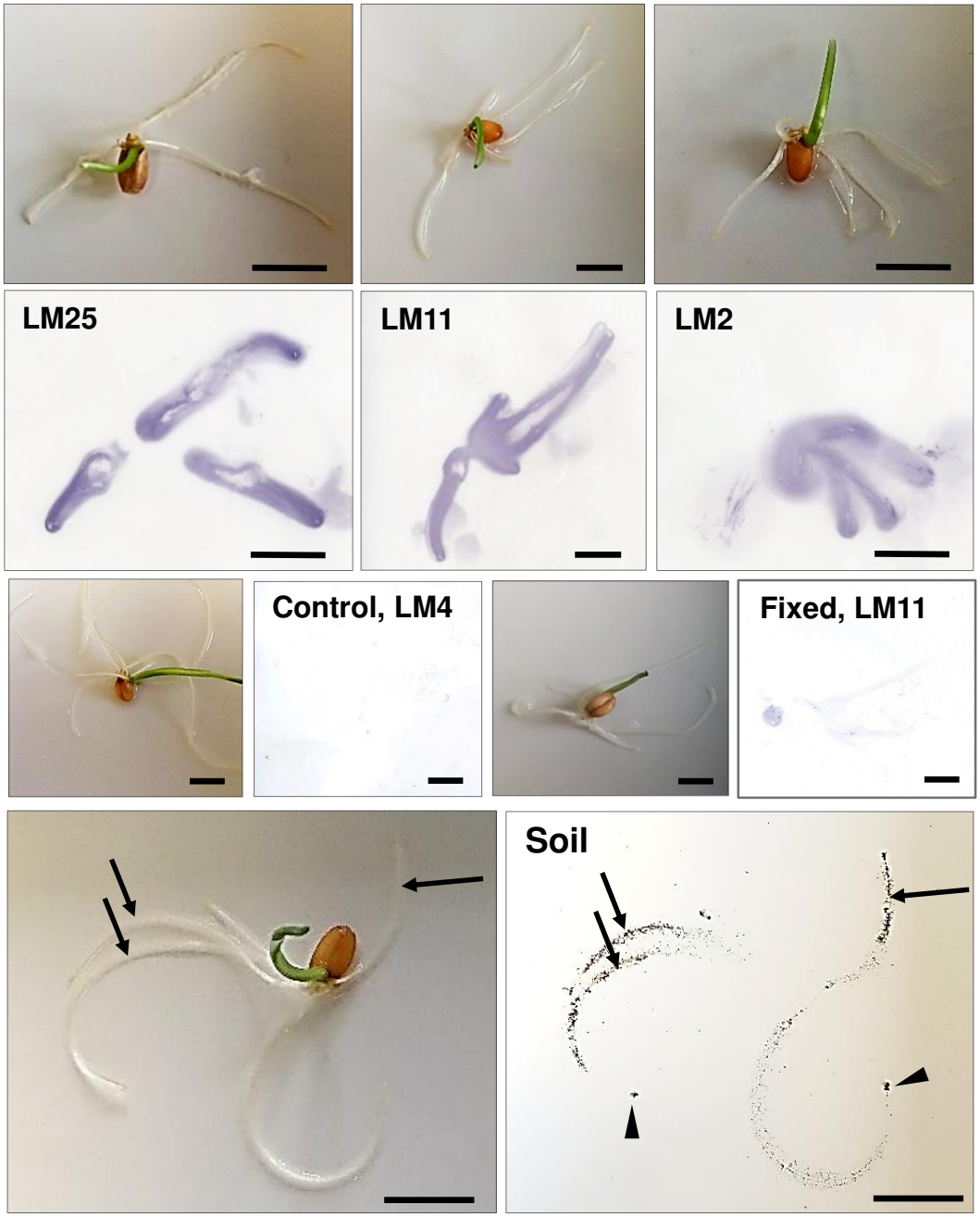

Fig. 4. Wheat seedlings release glycan epitopes present in HMW exudates and soil-binding factors along the root body. Top paired panels show wheat seedlings that were placed on nitrocellulose sheets for 2 h and associated probing of sheets with LM25 xyloglucan, LM11 xylan and LM2 AGP MAbs after seedling removal. Middle panels show the controls of irrelevant MAb LM4 (non-binding control) and loss of LM11 signal after pre-fixation of seedling. Bottom paired panels show a seedling and corresponding nitrocellulose sheet processed for the soil adhesion procedure (Akhtar et al. 2018). Arrows indicate root regions that released strong soil-binding molecules. Arrowheads indicate soil adhered at root tip positions. All nitrocellulose sheet images shown are representative of at least three replicates. Scale bars = 10 mm.

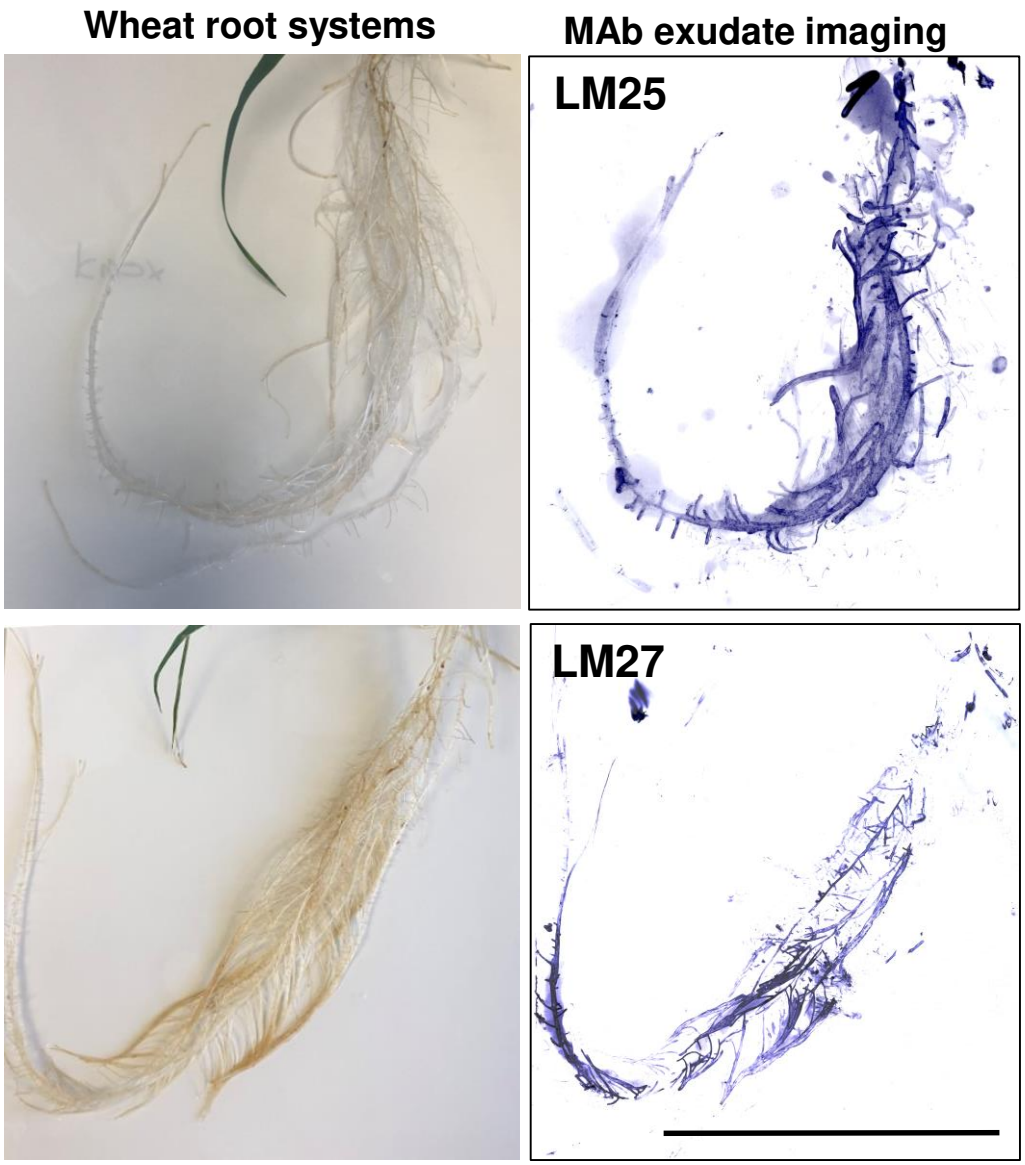

Fig. 5. Imaging of glycan epitopes in HMW exudates released from large wheat roots grown hydroponically for 2 weeks and then lain on sheets of nitrocellulose for 10 min prior to probing with MAbs. Images of root systems shown for the LM25 xyloglucan and the LM27 heteroxylan epitopes. All images scaled to the same extent and bar = 100 mm.

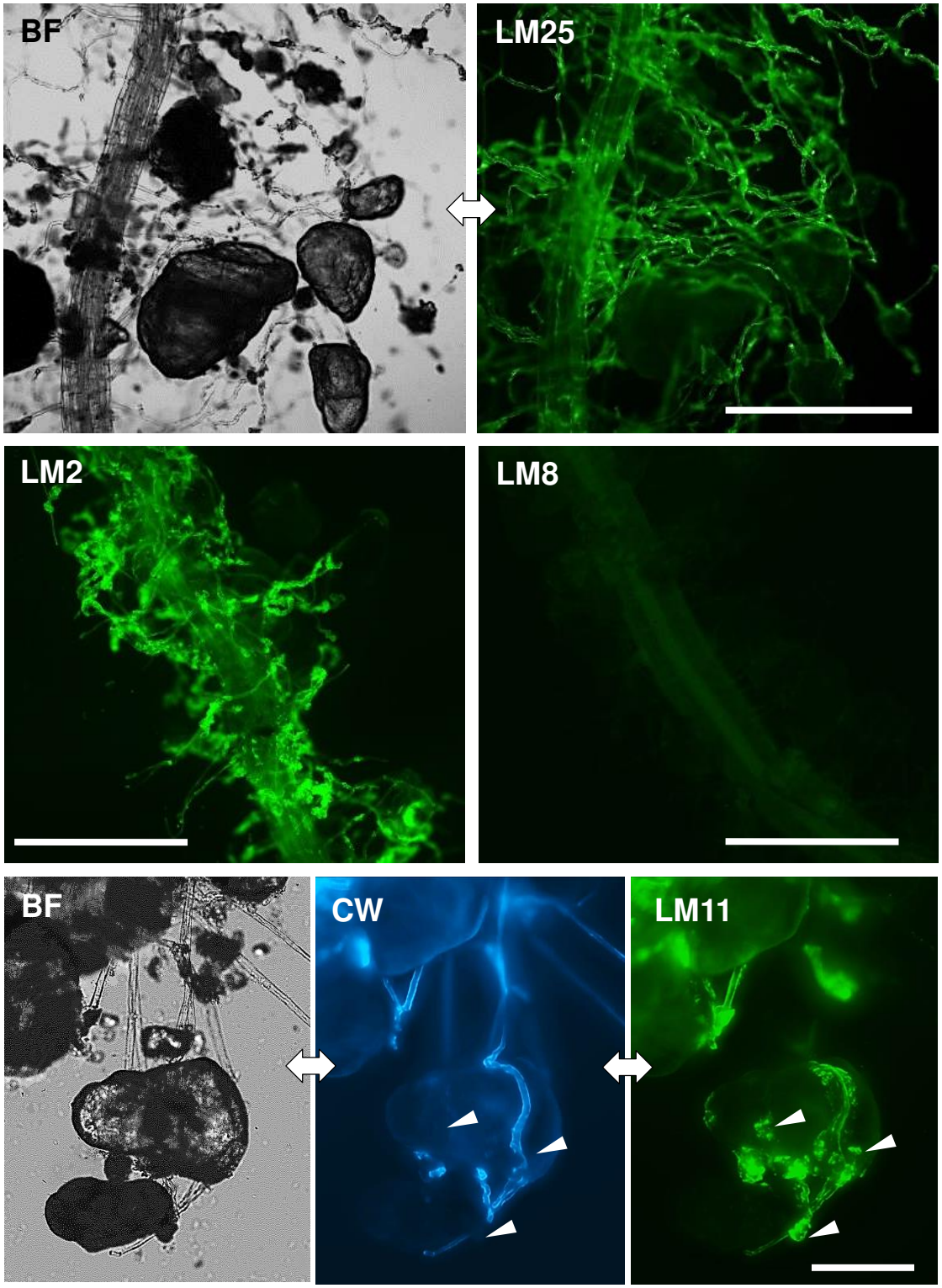

Fig. 6. Immunofluorescence detection in whole mount preparations of glycan epitopes on wheat root hairs in rhizosheaths. Top row: Paired bright field (BF) and LM25 xyloglucan immunofluorescence micrographs of the same region of rhizosheath soil attached to a wheat root. Bar = 500 µm. Middle row: Comparative immunofluorescence micrographs with LM2 AGP and LM8 xylogalacturonan (non-binding control) Mabs. Bars = 1 mm. Bottom row: Micrographs of soil particles attached to root hairs showing BF, Calcofluor White (CW) staining of cell walls and LM11 xylan epitope detection. Arrow heads indicate epitope detection on soil particle surfaces that are not part of cellulosic root hair cell walls. Bar = 200 µm.

Supplemental information Fig. 1. Rhizosheaths at the surface of wheat and maize roots. Plants were grown for 2 weeks in a soil-sand mix and watering stopped 3 days before harvest of root systems. Wheat seedlings retained 28.1 ± 9.7 g soil per g root fresh weight compared to maize roots (7.4 ± 2.0 g) across 6 biological replicates. Scale bars = 30 mm.